

Analytic model for planar growth of a solid germ from an undercooled melt

Ch. Charach* and B. Zaltzman†

*Center for Energy and Environmental Physics, Jacob Blaustein Institute for Desert Research,
Ben-Gurion University of the Negev, Sede-Boqer Campus, 84990 Israel*

(Received 1 November 1993)

Planar growth of a solid germ of infinitesimal initial thickness from an undercooled melt is addressed within a continuum model with linear interfacial kinetics. For this problem, we present an analytic solution that describes the global features of the process beyond the initial and long-time limits. In particular, it yields analytic expressions for the main characteristics of the transient regime. This solution is obtained within the heat balance integral method with a relatively simple boundary layer approximation for the temperature profile in the melt. The analytic solution is validated by the known asymptotic results, as well as by comparison with the numerical solution of the problem considered. The emerging physical picture is formulated in terms of the evolution characteristics of the phase-change front and those of the thermal boundary layer.

PACS number(s): 81.15.Lm, 61.50.Cj

I. INTRODUCTION

In recent years there has been considerable interest in the analysis of planar solidification of a pure substance from an undercooled melt. This problem has been addressed both within the continuum models with linear interfacial kinetics [1–6] as well as within the phase-field approach [7–9]. The main efforts so far have been devoted to analysis of the interface motion in the long-time regime.

The dynamics of the process depends on the level of initial undercooling parametrized by the Stefan number $St = c_L(T^* - T_\infty)/L^*$. Here, T^* and T_∞ stand for the equilibrium freezing point and the initial temperatures, respectively; L^* is the latent heat at the temperature $T = T^*$, and c_L is the liquid specific heat assumed to be constant. It is now well established that at long times the front $R(t)$ advances as \sqrt{t} for $St < 1$, as $t^{2/3}$ for $St = 1$, and as t for $St > 1$. (Within the phase-field models, constant velocity of the front is also allowed under certain conditions dictated by the microscopic considerations.)

In order to obtain more detailed information concerning the advance of the interface at short and intermediate times, as well as the temperature fields, several asymptotic and numerical solutions have been developed [2,5–9]. Clearly, the nature of these solutions depends on the initial conditions imposed. In a recent paper [5] we addressed a typical problem of this sort, describing the growth of a solid germ of infinitesimal initial thickness and developing the short-time and long-time asymptotic solutions both for the interface advance and for the corresponding temperature profiles. Some results of numeri-

cal studies of this problem have been recently given in [6].

The aim of the present paper is to go beyond the asymptotic analysis of [5] by developing a sufficiently simple and physically transparent analytic solution, valid uniformly in time. Such a solution would also clarify the main features of the transient regime, such as the characteristic times required to establish the long-time asymptotic states.

For this purpose we adopt here the heat balance method [10,11], which replaces the heat diffusion equations by their zero order moments with assumed spatial dependence of the temperature profiles. The physics behind the selection of these profiles determines the adequacy of such a solution. Once the profiles are fixed, the problem reduces to a set of ordinary differential equations for characteristic functions parametrizing the temperature profiles. Some years ago, such a method was used for the problem of isothermal solidification of alloys (with rather complicated nonlinear interfacial kinetics, but without the solute trapping effects), assuming a linear concentration profile of variable thickness [12]. More recently, such a method has been applied to several transient problems of directional solidification [13,14] using a relatively simple boundary layer approximation for the concentration profiles. These profiles are of the same form as the long-time asymptotic solutions for the temperature field obtained in [5] for $St \geq 1$.

The present paper implements the heat balance integral method for the problem considered by adopting the boundary layer approximation for the temperature profiles in the entire range $0 < t < \infty$. It is demonstrated that the solution developed in this way reproduces with a reasonable accuracy the main features of the numerical studies of the problem in its full generality. The emerging physical picture of the process is formulated in terms of the monotonic relaxation of the interface temperature to its limiting value, determined by the undercooling parameter St , and the rate of expansion of the thermal boundary layer versus that of advance of the solidification front.

*Also at Department of Physics, Ben-Gurion University of the Negev, Beer-Sheva, Israel.

†Also at Department of Mathematics and Computer Science, Ben-Gurion University of the Negev, Beer-Sheva, Israel.

II. STATEMENT OF THE PROBLEM WITHIN THE HEAT BALANCE INTEGRAL METHOD

Following [5], let us consider a uniformly undercooled melt at the temperature $T_L(0, x) = T_\infty < T^*$, occupying an infinite space. At time $t=0$, a planar solid germ of infinitesimal thickness has nucleated at $x=0$. Its initial temperature $T_S(0, 0)$ is equal to T_∞ . We assume that the growth of this germ is planar and symmetric with respect to the $x=0$ plane. Within the continuum model with linear interfacial kinetics, the problem is stated as follows:

$$T_{S,t} = \alpha_S T_{S,xx}, \quad 0 < x < R(t), \quad (1)$$

$$T_{L,t} = \alpha_L T_{L,xx}, \quad R(t) < x < \infty. \quad (2)$$

$$T_{L|x=R} = T_{S|x=R} = T_c = T^* - av, \quad v \equiv \frac{dR}{dt}. \quad (3)$$

$$\rho_L v = k_S T_{S,x|x=R} - k_L T_{L,x|x=R}, \quad L = L^* [1 - av(c_L - c_S)], \quad (4)$$

$$T_L(0, x) = T(t, \infty) = T_\infty, \quad T_{S,x|x=0} = T_{L,x|x=\infty} = 0, \quad R(0) = 0. \quad (5)$$

Here, the subscripts L and S denote the liquid and the solid, respectively; k is the thermal conductivity; $\alpha = k/\rho c$ is the thermal diffusivity; $\rho_L = \rho_S = \rho$ is the density; c is the specific heat; and a is the kinetic coefficient ($a > 0$).

In order to develop an approximate analytic solution of this problem within the heat balance integral method, we integrate the diffusion equations (1) and (2) with respect to x :

$$\frac{d}{dt} \int_0^R T_S(x, t) dx - v T_c - \alpha_S T_{S,x|x=R}, \quad (6)$$

$$\frac{d}{dt} \int_R^\infty T_L(x, t) dx - v T_c = -\alpha_L T_{L,x|x=R}. \quad (7)$$

For the sake of simplicity, we disregard the nonuniformity of the solid temperature assuming $T_S(x, t) = T_c$ for $0 \leq x \leq R(t)$. This assumption is consistent both with the short-time and with the long-time asymptotic solutions developed in [5]. Under the latter assumption, Eqs. (3)–(5) and (7) yield

$$\frac{d}{dt} \int_R^\infty (T_L - T_\infty) dx = (1 - St) \frac{L^*}{c_L} v - acv^2. \quad (8)$$

Here, $c = c_L/c_S$.

The next step in implementation of the heat balance integral method is the selection of the temperature profiles of the undercooled melt. For the case $St < 1$, we assume

$$T_L(x, t) = T_\infty + (T_c - T_\infty) \frac{\operatorname{erfc}\{\Omega[1 + (x - R)/l]\}}{\operatorname{erfc}\Omega}, \quad (9)$$

where Ω is the root of the transcendental equation

$$\sqrt{\pi} \Omega \exp(\Omega^2) \operatorname{erfc}\Omega = St \quad (10)$$

and $l = l(t)$ is the time-dependent length scale of decay of the liquid temperature. Its value is determined by the interfacial heat balance, Eq. (4):

$$l(t) = \frac{2\Omega^2 \alpha_L c_L (T_c - T_\infty)}{St v L}. \quad (11)$$

From Eq. (10) and the asymptotic expansions of the error function [15], it follows that for $St \ll 1$, in the leading order, $\Omega \approx St/\sqrt{\pi}$, whereas for $1 - St \ll 1$, $\Omega \approx 1/\sqrt{2(1 - St)}$.

According to [5], at long times T_c tends to T^* and the interface advance in this diffusion-dominated regime is governed by $R(t) \approx 2\Omega\sqrt{\alpha_L t}$. Therefore, as $t \rightarrow \infty$, $l(t)/R(t)$ tends to unity, and the liquid temperature profile, given by Eq. (9), tends to the asymptotic solution of the corresponding Stefan problem [15]. Notice that the assumed temperature profile, Eq. (9), satisfies also the initial condition at $t=0$.

For $St \geq 1$, we approximate the liquid temperature profile by

$$T_L(x, t) = T_\infty + (T_c - T_\infty) \exp\left[-\frac{x - R}{l}\right]. \quad (12)$$

Here, $l(t)$ is again the time-dependent length scale of the liquid temperature decay. Its value is given by

$$l(t) = \frac{\alpha_L c_L (T_c - T_\infty)}{v L}. \quad (13)$$

In the long-time limit, Eqs. (12) and (13) reproduce the asymptotic solutions for T_L developed in [5]. The profiles (12), describing a boundary layer with a time-dependent thickness, are of the same form as those used in transient directional solidification problems discussed by Warren and Langer [13] and by Caroli, Caroli, and Ramirez-Piscina [14].

We now insert the above temperature profiles into the heat balance equation (8) using the scaled variables $\tau \equiv t/t_0$, $w \equiv v/v_0$, with

$$v_0 = \frac{(T^* - T_\infty)}{a} \equiv v|_{t=0}, \quad t_0 \equiv \frac{\alpha_L}{v_0^2}. \quad (14)$$

This yields the following equation for the interface acceleration:

$$\frac{dw}{d\tau} = \frac{w^3 f(1 - St'w) \left[(1 - St) + \frac{wSt}{c} \right]}{w^2 - 1 + 2St'w(1 - w)}, \quad (15)$$

with the initial condition $w(0) = 1$. Here, f is a continuous function of the undercooling parameter St , given by

$$f = \begin{cases} \frac{1}{2\Omega^2(1 - St)} & \text{if } St < 1 \\ \frac{1}{St^2} & \text{if } St \geq 1, \end{cases} \quad (16)$$

and $St' = St(c - 1)/c$. Usually, c is very close to unity, and the validity of the linear approximation for the inter-

facial kinetics, adopted in this paper, implies that for relevant situations $St' < 1$.

Thus the original solidification problem, defined by Eqs. (1)–(5), has been reduced to the initial value problem for the ordinary differential equation (15). Once this problem is solved, the interface position R can be found by direct integration:

$$R = \frac{\alpha_L}{v_0} \int_1^w w \left(\frac{dw}{d\tau} \right)^{-1} d\tau. \quad (15')$$

III. APPROXIMATE SOLUTION: INTERFACE MOTION

Let us now analyze the interface advance as defined by Eq. (15). First we prove that the interface velocity is monotonically decreasing in time and define the asymptotic attractors of the problem. To begin with, let us examine the onset of freezing, when w is sufficiently close to its initial value $w(0) = 1$. In this regime Eq. (15) yields

$$w(\tau) = 1 \pm \sqrt{f(1 - St')\tau} + O(\tau). \quad (17)$$

Positive initial velocity of the front and the local heat balance at the interface, Eq. (4), along with the assumption $T_S = T_c$, imply that at the onset of freezing $\partial T_L / \partial x$ is negative. This means that the heat liberated at the interface is emitted into the liquid. Consequently, the interface temperature T_c is increasing in time. Therefore, for sufficiently short times, the interface velocity is decreasing in time. This dictates selection of the minus sign in Eq. (17). Once $w < 1$, the right-hand side (rhs) of Eq. (15) is negative as long as $w_\infty < w \leq 1$, where $w_\infty = 0$ for $St \leq 1$, and $w_\infty = c(St - 1)/St$ for $St > 1$. Thus the solidification process is accompanied by monotonic relaxation of the front velocity to its limiting values w_∞ , determined by the initial undercooling parameter St . By direct integration of Eq. (15), it can be shown that these states serve as asymptotic attractors when $t \rightarrow \infty$.

The short-time asymptotics of the interface velocity, defined by Eq. (17), resembles that given in [5]: $1 - w(\tau) = B\sqrt{\tau} + O(\tau)$, although the value of B in [5] differs from $\sqrt{f(1 - St')}$. Equation (15) reproduces correctly the long-time asymptotics of the interface motion: For $St > 1$, w tends to a constant value $c(St - 1)/St$; for $St = 1$, $w \approx (c/3\tau)^{1/3}$ when $\tau \rightarrow \infty$; and for $St < 1$, the long-time behavior of w is given by $w \approx \Omega/\sqrt{\tau}$. Thus we have shown the consistency of the present model with the earlier asymptotic studies discussed in [5].

Equation (15) determines the interface motion for the entire range $0 < t < \infty$, extending analysis beyond the short-time and the long-time asymptotics. This allows one to study the typical behavior of the process considered in the transient regime. Direct integration of Eq. (15) is straightforward, although the resulting expressions are rather lengthy. For the sake of simplicity, from now on we restrict the discussion to the case $c = 1$. Then integration of Eq. (15) yields

$$\begin{aligned} \tau f(St - 1) = & \frac{1}{2}(1 - w^{-2}) + \frac{St}{St - 1}(1 - w^{-1}) \\ & + \frac{1 - 2St}{(St - 1)^2} \ln \left| \frac{St - 1 - wSt}{w} \right|. \end{aligned} \quad (18)$$

Notice that $\tau(w, St)$ is a continuous function of St , and for $St = 1$, Eq. (18) reduces to a simple expression:

$$\tau = \frac{2}{3} - \frac{1}{w} + \frac{1}{3w^3}. \quad (19)$$

We can now estimate the duration of the transient regime, $\tau_{rel} = \tau(w_{rel}, St)$. For $St \leq 1$, τ_{rel} is defined as the time τ , at which the interface velocity w drops to the value

$$w_{rel} = w_\infty + 0.1(1 - w_\infty).$$

For $St \leq 1$, $\tau_{rel} = \tau(0.1, St)$, and for $St > 1$,

$$\tau_{rel} = \tau[w = (St - 0.9)/St, St].$$

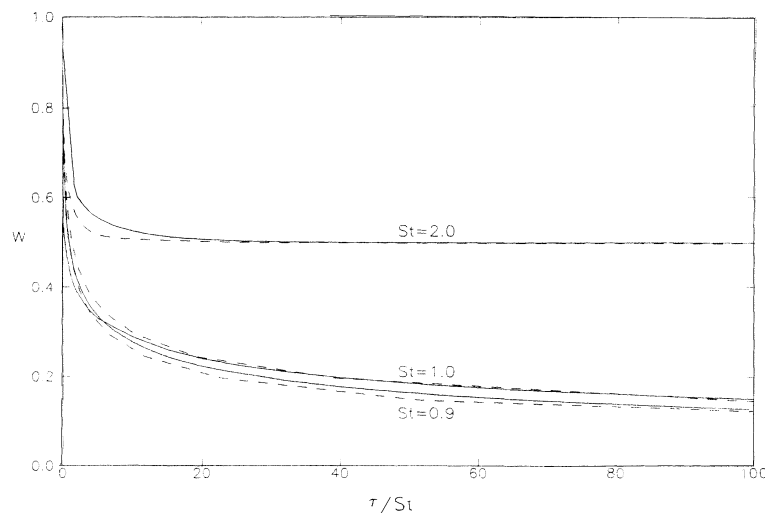


FIG. 1. The dimensionless velocity of the interface, $w(\tau)$, as a function of dimensionless time τ for $\alpha_L = \alpha_S$, and $c = 1$: Solid lines, numerical solution; dashed lines, analytic solution.

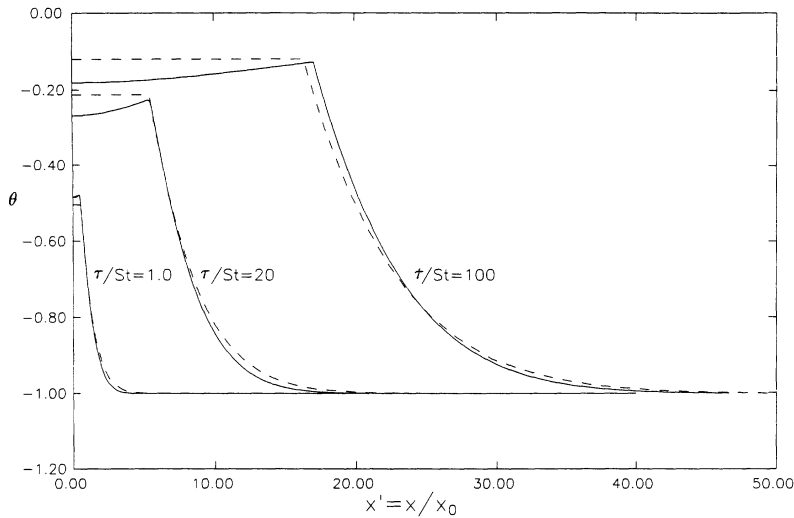


FIG. 2. Dimensionless temperature $\theta(\tau, x') = T - T^* / T^* - T_\infty$ as a function of dimensionless spatial coordinate $x' = x/x_0$ for $St = 0.9$, and $\alpha_L = \alpha_S$, and $c = 1$: Solid lines, numerical solution; dashed lines, analytic solution.

It follows, from Eq. (18), that the duration of the transient regime is significantly affected by the level of initial undercooling. While the transients are short lived for $St \ll 1$, or for St of the order 10, τ_{rel} increases when $St \rightarrow 1$ both from above and from below. This observation is in accord with the numerical studies performed within the phase-field model [8]. Maximal duration of the transient corresponds to the critical undercooling, $St = 1$, for which Eq. (19) yields $\tau_{rel} = 324$.

In Fig. 1 we present graphs of $w = w(\tau, St)$, calculated using Eqs. (18) and (19) for several values of the parameter St . For comparison, the corresponding curves, obtained by numerical solution [6] of the full problem, as stated by Eqs. (1)–(5), are presented for $c = 1$ and $\alpha_S = \alpha_L$. It follows that the approximate analytic solution developed above reproduces with a reasonable accuracy the main features of the numerical solution of the actual problem.

IV. TEMPERATURE PROFILES

Let us now consider the implications of the results of Sec. III on the evolution of the temperature profiles (9)

and (12). Due to continuous liberation of latent heat, the interface temperature is monotonically increasing in time. For $St \leq 1$, T_c tends to its equilibrium value T^* , whereas for $St > 1$, T_c increases towards its asymptotic value

$$T^* - av_0[(St - 1)/St].$$

The temperature profiles (9) and (12) describe the thermal boundary layers, the thickness of which is varying in time. Within the present model, this thickness is one of the major evolution characteristics of the problem. Since the rate of growth of a solid differs from that of the "boundary layer spreading," the ratio $l(t)/R(t)$ is another important characteristic of the present solution. In order to study these characteristics, it is convenient to express the spatial scale $l(t)$, given by Eqs. (11) and (13), as

$$\frac{l(t)}{x_0} = \begin{cases} St \frac{1-w}{w} & \text{if } St \geq 1 \\ 2\Omega^2 \frac{1-w}{w} & \text{if } St < 1, \end{cases} \quad (20)$$

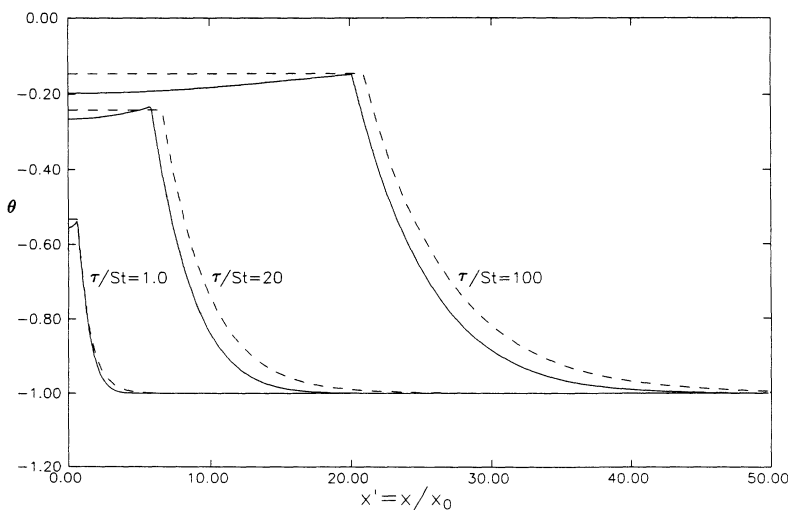


FIG. 3. Dimensionless temperature $\theta(\tau, x') = T - T^* / T^* - T_\infty$ as a function of dimensionless spatial coordinate $x' = x/x_0$ for $St = 1.0$, $\alpha_L = \alpha_S$, and $c = 1$: Solid lines, numerical solution; dashed lines, analytic solution.

where $x_0 = \alpha_L / v_0$. According to Eq. (20), $l(t)$ is monotonically increasing in time, due to the continuous deceleration of the interface. Notice that for $St \geq 1$ the spatial decay of T_c is exponential, and $l(t)$ is the actual width of the thermal boundary layer. For $St < 1$, where the melt temperature is given in terms of the error functions, the situation is more complicated: Although $l(t)$ still characterizes the spatial decay of $T_L(x, t)$, the actual

width of the boundary layer depends on the value of parameter St in a more complicated fashion. For instance, when $\Omega \ll 1$ ($St \ll 1$), $l' = l/\Omega$ is the length scale at which the melt temperature $T_L(x, t)$ drops roughly by a factor 6 from its maximal value $T_c(t)$. For large values of Ω , i.e., $1 - St \ll 1$, the melt temperature can be approximated by

$$T_L \approx T_\infty + (T_c - T_\infty) \frac{\exp[-(x - R)/l''] \exp\{-(x - R)^2/[4\Omega^2(l'')^2]\}}{1 + (x - R)/l} \tag{21}$$

where $l'' = l/2\Omega^2$. In this case, l'' serves as the natural width of the boundary layer.

Let us now examine the behavior of $l(t)$ and $l(t)/R(t)$ in the limits $\tau \rightarrow 0$ and $\tau \rightarrow \infty$. For short times,

$$\frac{l(t)}{x_0} \approx \begin{cases} \sqrt{\tau} & \text{if } St \geq 1 \\ \Omega \left[\frac{2\tau}{1 - St} \right]^{1/2} & \text{if } St < 1, \end{cases} \tag{22}$$

and the ratio $l(t)/R(t)$ blows up as $1/\sqrt{\tau}$ when $\tau \rightarrow 0$.

In the course of the process $l(t)$ grows indefinitely for $St \leq 1$, whereas it tends to a constant value for $St > 1$. For long times,

$$\frac{l(t)}{x_0} \approx \begin{cases} 2\Omega\sqrt{\tau} & \text{if } St < 1 \\ (3\tau)^{1/3} & \text{if } St = 1 \\ \frac{St}{St - 1} & \text{if } St > 1, \end{cases} \tag{23}$$

and the ratio l/R is given by

$$\frac{l(t)}{R(t)} \approx \begin{cases} 1 & \text{if } St < 1 \\ \frac{2}{(3\tau)^{1/3}} & \text{if } St = 1 \\ \frac{St^2}{(St - 1)^2\tau} & \text{if } St > 1. \end{cases} \tag{24}$$

To this end, we present in Figs. 2-4 the temperature profiles of T_L calculated using the approximate solution, derived above for $c = 1$ and $St = 0.9, 1.0$, and 2.0 , respectively, and compare them with the corresponding results of the numerical solution of the full problem as stated in Eqs. (1)-(5). These figures indicate that the approximate analytic solution, based on the heat balance integral method, reproduces correctly the qualitative features of the temperature field and that the quantitative agreement between the approximate and numerical solutions is also reasonably good.

V. CONCLUDING REMARKS

We developed above an approximate analytic solution for planar growth of a solid germ from a uniformly undercooled melt. This solution is in agreement with the

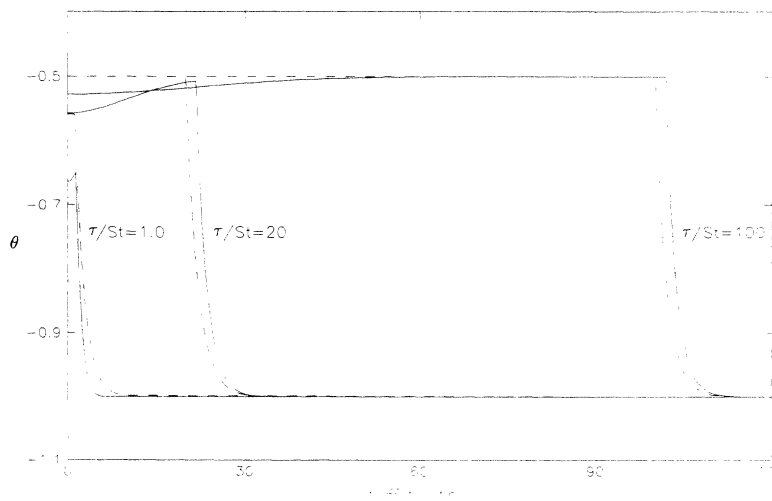


FIG. 4. Dimensionless temperature $\theta(\tau, x') = T - T^* / T^* - T_\infty$ as a function of dimensionless spatial coordinate $x' = x/x_0$ for $St = 2.0$, $\alpha_L = \alpha_S$, and $c = 1$: Solid lines, numerical solution; dashed lines, analytic solution.

previously found asymptotic solutions [5] and reproduces, with a reasonable accuracy, the numerical results given in [6]. Being valid for the entire range $0 < t < \infty$, the present solution is also adequate in the transient stage of the solidification process. Furthermore, the relative simplicity of this solution yields a rather transparent physical interpretation of the process in terms of the front propagation and evolution of the thermal boundary layer in the melt.

The physical picture emerging from this model is as follows: The solidification rate is monotonically decreasing in time. Simultaneously continuous liberation of latent heat raises the interface temperature. Both the width of the solid germ and the thickness of the thermal boundary layer, produced in the melt due to the diffusion of heat emitted at the interface, are constantly increasing in time. However, the solidification rate differs from the rate of spreading of the boundary layer. At short times the thickness of the thermal boundary layer is far greater than the size of the solid germ, and $l(\tau)/R(\tau) \sim 1/\sqrt{\tau}$ as $\tau \rightarrow 0$, for any value of the parameter St . In the course of the process l/R is monotonically decreasing and its long-time behavior is determined by the level of initial undercooling.

For $St < 1$ the diffusion-controlled Stefan solution [15] serves as the long-time attractor of the present solution. For long times both the rate of growth of the thermal

boundary layer and that of the solid germ follow the diffusion law: $l(\tau) \sim R(\tau) \sim \sqrt{\tau}$. As $St \rightarrow 1$, the duration of the transient stage increases, and the temperature profile resembles a plane wave, propagating with a time-dependent velocity $w \sim 1/\sqrt{\tau}$. For critical undercooling, $St = 1$, the relaxation of T_c towards its equilibrium value T^* is very slow: τ_{rel} is of the order 300. For long times the rate of solidification is greater than that of the thermal boundary layer spreading and $l(\tau)/R(\tau)$ drops as $\tau^{-1/3}$ when $\tau \rightarrow \infty$. Finally, in the kinetics-controlled case, $St > 1$, the interface temperature is always below T^* . For long times, the solution is of the traveling wave type [1] propagating with a constant velocity v_∞ proportional to $(St-1)/St$. In that case the width of the thermal boundary layer tends towards the constant value α_L/v_∞ . Again, the duration of the transient stage increases when $St \rightarrow 1$ from above.

The approximate method, utilized in the present paper, involves the temperature profile, parametrized by two functions $R(t)$ and $l(t)$, which are coupled via the interfacial heat balance and the zero order moment of the heat diffusion equation. Improvement of the accuracy of this method is still an open question. It seems that this issue might be addressed using the temperature profiles with more freedom, supplemented by the higher order moments of the diffusion equation, and subdivision of the spatial domain in the spirit of the finite element method.

-
- [1] M. E. Glicksman and R. J. Shaefer, *J. Cryst. Growth* **1**, 297 (1967).
- [2] A. Umantsev, *Kristallografiya* **30**, 153 (1985) [*Sov. Phys. Crystallogr.* **30**, 87 (1985)].
- [3] J. N. Dewynne, S. D. Howison, J. R. Ockendon, and Weiqing Xie, *J. Aust. Math. Soc. B* **31**, 81 (1989).
- [4] P. Oswald (unpublished), cited in H. Löwen, J. Bechhoefer, and L. Tuckerman, *Phys. Rev. A* **45**, 2399 (1992).
- [5] Ch. Charach and B. Zaltzman, *Phys. Rev. E* **47**, 1230 (1993).
- [6] Ch. Charach and B. Zaltzman, in *Computational Modeling of Free and Moving Boundary Problems*, edited by L. C. Wrobel and C. A. Brebbia (Computational Mechanics Publications, Southampton, 1993).
- [7] H. Löwen, S. A. Schoefield, and D. W. Oxtoby, *J. Chem. Phys.* **94**, 5685 (1991).
- [8] H. Löwen, J. Bechhoefer, and L. Tuckerman, *Phys. Rev. A* **45**, 2399 (1992).
- [9] M. Marder, *Phys. Rev. A* **45**, R2158 (1992).
- [10] T. R. Goodman, *ASME J. Heat Transfer* **83**, 83 (1961).
- [11] Ch. Charach and P. Zoglin, *Int. J. Heat Mass Transfer* **28**, 2261 (1985).
- [12] G. M. Kudinov, D. Ye. Temkin, and Y. A. Lyubov, *Fiz. Met. Metalloved.* **46**, 540 (1978).
- [13] J. M. Warren and J. S. Langer, *Phys. Rev. E* **47**, 2702 (1993).
- [14] B. Caroli, C. Caroli, and L. Ramirez-Piscina, *J. Cryst. Growth* **132**, 377 (1993).
- [15] H. S. Carslaw and J. S. Jaeger, *Conduction of Heat in Solids* (Oxford University Press, Oxford, 1959).